한국소음진동공학회 1997년도 춘계학술대회논문집, pp. 110 ~ 115.

동적문제 해석을 위한 사다리꼴 시간적분법의 일반화

0 조진연*, 김승조*

A Generalization of the Trapezoidal Rule for Dynamic Analysis

Jin Yeon Cho, Seung Jo Kim

ABSTRACT

In this work, the constant average acceleration, which is a fundamental feature of the trapezoidal rule, is investigated and generalized. Using the generalization of average acceleration concept, a higher order accurate and unconditionally stable time-integration method is developed. The linear approximation of the present method is exactly the same as the famous trapezoidal rule.

To observe the accuracy and stability of the method, several numerical tests are performed and the results are compared with the results from the trapezoidal rule and the exact solution. From the numerical tests, it has been known that the present method has a higher order accuracy and unconditional stability.

I. Introduction

Over many years, numerous numerical time-integration algorithms[1-7] have been developed for structural dynamics. These methods have different characteristics of accuracy, stability and numerical dissipation[8]. Each of these numerical time-integration methods has its specialty for a specific problem. However, for general purposes, the Newmark family algorithm is one of the most widely used methods in structural dynamics. As special cases, it contains many well-known and widely used methods. The most famous form of the Newmark family is the trapezoidal rule which was proposed originally as the constant average acceleration method by Newmark[1]. It was proved by Dahlquist[9] that the trapezoidal rule has the smallest error in the unconditionally stable linear multi-step methods, having the second-order accuracy. In this work, the trapezoidal rule is generalized to develop the higher order accurate and unconditionally stable time-integration method.

II. Theory

1. Generalized Averages for Acceleration and Velocity

The linear space $P_\alpha^k[t_n, t_{n+1}]$ of vector valued function $\mathbf{p}(t) = (p_1(t), p_2(t), \cdots, p_k(t))^T$ elements of which are real polynomial of degree less than or equal to α defined over an interval $t_n \le t \le t_{n+1}$, with the inner product defined as

$$(\mathbf{p}, \mathbf{q}) = \int_{t_n}^{t_{n+1}} \mathbf{p}(t)^T \mathbf{q}(t) dt \qquad (1)$$

is an inner product space. Since $P_\alpha^k[t_n, t_{n+1}]$ is a finite dimensional linear space, it is complete[10]. Hence, it is a Hilbert space. Moreover, it can be easily shown that $P_i^k[t_n, t_{n+1}]$ for $0 \le i < \alpha$ is a closed linear subspace of $P_\alpha^k[t_n, t_{n+1}]$. Thus the projection theorem[11] can be applied. From the projection theorem, the closest vector $\bar{\mathbf{p}}(t) \in P_{\alpha-1}^k[t_n, t_{n+1}]$ to the vector $\mathbf{p}(t) \in P_\alpha^k[t_n, t_{n+1}]$ can be found. It corresponds to the orthogonal projection of $\mathbf{p}(t)$, where the range space of orthogonal projection operator is $P_{\alpha-1}^k[t_n, t_{n+1}]$. The closest vector $\bar{\mathbf{p}}(t)$ is obtained as follows.

$$\begin{aligned} &\textit{For the given } \mathbf{p}(t) \in P_\alpha^k[t_n, t_{n+1}], \\ &\textit{Find } \bar{\mathbf{p}}(t) \in P_{\alpha-1}^k[t_n, t_{n+1}] \textit{ such that} \\ &(\mathbf{p} - \bar{\mathbf{p}}, \mathbf{q}) = 0, \textit{ for all } \mathbf{q}(t) \in P_{\alpha-1}^k[t_n, t_{n+1}] \end{aligned} \qquad (2)$$

Actually, the constant average of a vector valued linear function(k–tuple of linear polynomials) can be understood mathematically to be the vector valued constant polynomial (k–tuple of constant polynomials) which is the closest to the vector valued linear function in the constant polynomial space $P_o^k[t_n, t_{n+1}]$. It is also considered as the orthogonal projection of the linear function vector to constant polynomial space $P_o^k[t_n, t_{n+1}]$. Similarly, the vector valued higher order polynomial functions(k–tuple of higher order polynomials) can be averaged to one-degree lower order polynomial function in the above

* Department of Aerospace Engineering
Seoul National University

sense. By the same way, the averages of higher order acceleration and velocity can be derived.

The α-th order acceleration vector defined on an interval $t_n \le t \le t_{n+1} = (t_n + \Delta t)$ is written in the following form by using Lagrange interpolation functions.

$$\mathbf{a}(t) = \sum_{i=0}^{\alpha} \psi_i(t)\mathbf{a}_{n+i/\alpha} \tag{3}$$

where $\Delta t = (t_{n+1} - t_n)$ is time step and $n + i/\alpha$ denotes the time of i-th inner time step ($t_n < t_{n+1/\alpha} < t_{n+2/\alpha} < \cdots < t_{n+(\alpha-1)/\alpha} < t_{n+1}$). The inner time step $(t_{n+(i+1)/\alpha} - t_{n+i/\alpha})$ is $\Delta t/\alpha$ for all $0 \le i \le (\alpha - 1)$.

To find the averaged value $\bar{\mathbf{a}}(t) \in P_{\alpha-1}^k[t_n, t_{n+1}]$ for $\mathbf{a}(t) \in P_\alpha^k[t_n, t_{n+1}]$, it is sufficient to solve the following relation.

$$(\mathbf{a} - \bar{\mathbf{a}}, \mathbf{q}) = 0, \textit{ for all } \mathbf{q}(t) \in P_{\alpha-1}^k[t_n, t_{n+1}] \tag{4}$$

It is equivalent to finding the polynomial vector $\bar{\mathbf{a}}(t) \in P_{\alpha-1}^k[t_n, t_{n+1}]$ such that

$$\bar{\mathbf{a}}(t) = \sum_{i=0}^{\alpha} \bar{\psi}_i(t)\mathbf{a}_{n+i/\alpha} \tag{5}$$

where $\bar{\psi}_i(t)$ is the polynomial of $\alpha - 1$ degree and satisfies

$$\int_{t_n}^{t_{n+1}} [\psi_i(t) - \bar{\psi}_i(t)]t^j dt = 0, \textit{ for all } 0 \le j \le \alpha - 1 \tag{6}$$

The velocity vector is obtained from the averaged acceleration vector by integration.

$$\mathbf{v}(t) = \int_{t_n}^{t} \bar{\mathbf{a}}(t)dt + \mathbf{v}_n = \sum_{j=0}^{\alpha} \psi_j(t)\mathbf{v}_{n+j/\alpha} \tag{7}$$

The relation between acceleration and velocity at each inner time step can be obtained by

$$\mathbf{v}_{n+i/\alpha} = \int_{t_n}^{t_{n+i/\alpha}} \bar{\mathbf{a}}(t)dt + \mathbf{v}_n = \sum_{j=0}^{\alpha} \left\{ \int_{t_n}^{t_{n+i/\alpha}} \bar{\psi}_j(t)dt \right\} \mathbf{a}_{n+j/\alpha} + \mathbf{v}_n \tag{8}$$

It can be rewritten in simplified matrix form as

$$\mathbf{V}_{n+1} = \bar{\Psi}\mathbf{A}_{n+1} + \bar{\Psi}_o\mathbf{A}_n + \mathbf{J}\mathbf{V}_n \tag{9}$$

where $\mathbf{V}_{n+1} = \{\mathbf{v}_{n+1/\alpha}^T, \mathbf{v}_{n+2/\alpha}^T, \cdots, \mathbf{v}_{n+1}^T\}^T$

$\mathbf{A}_{n+1} = \{\mathbf{a}_{n+1/\alpha}^T, \mathbf{a}_{n+2/\alpha}^T, \cdots, \mathbf{a}_{n+1}^T\}^T$

By the same procedure, the averaged velocity $\bar{\mathbf{v}}(t) \in P_{\alpha-1}^k[t_n, t_{n+1}]$ is given as

$$\bar{\mathbf{v}}(t) = \sum_{i=0}^{\alpha} \bar{\psi}_i(t)\mathbf{v}_{n+i/\alpha} \tag{10}$$

The displacement vector is recovered from the averaged velocity vector by integration. It can be rewritten in simplified matrix form

$$\mathbf{U}_{n+1} = \bar{\Psi}\mathbf{V}_{n+1} + \bar{\Psi}_o\mathbf{V}_n + \mathbf{J}\mathbf{U}_n \tag{11}$$

where $\mathbf{U}_{n+1} = \{\mathbf{u}_{n+1/\alpha}^T, \mathbf{u}_{n+2/\alpha}^T, \cdots, \mathbf{u}_{n+1}^T\}^T$

The obtained relations for displacement-velocity and velocity-acceleration are used for time integration with the dynamic equilibrium equations like the trapezoidal rule.

2. Time Integration Algorithm

Addition to the relations for displacement-velocity and velocity-acceleration, the dynamic equilibrium equations at the inner time steps $t_{n+i/\alpha}$ are considered to obtain a time integration algorithm.

$$\mathbf{m}\mathbf{a}_{n+i/\alpha} + \mathbf{c}\mathbf{v}_{n+i/\alpha} + \mathbf{k}\mathbf{u}_{n+i/\alpha} = \mathbf{f}_{n+i/\alpha}, \quad 1 \le i \le \alpha \tag{12}$$

In simplified matrix notation, it can be denoted as

$$\mathbf{M}\mathbf{A}_{n+1} + \mathbf{C}\mathbf{V}_{n+1} + \mathbf{K}\mathbf{U}_{n+1} = \mathbf{F}_{n+1} \tag{13}$$

where **M**,**C** and **K** are block diagonal matrices for mass, damping, and stiffness, respectively and **F** denotes the forcing vector.

For obtaining the unknowns $\mathbf{A}_{n+1}, \mathbf{V}_{n+1}, \mathbf{U}_{n+1}$, it is sufficient to solve the equations (9), (11), and (13), simultaneously. Thus the numerical time integration algorithm is reduced to obtain the solutions of the simultaneous algebraic equations. It is written by

For the given initial conditions $\mathbf{A}_n, \mathbf{V}_n, \mathbf{U}_n$,

find $\mathbf{A}_{n+1}, \mathbf{V}_{n+1}, \mathbf{U}_{n+1}$ *of the next time step such that*

$$\begin{aligned} \mathbf{V}_{n+1} &= \bar{\Psi}\mathbf{A}_{n+1} + \bar{\Psi}_o\mathbf{A}_n + \mathbf{J}\mathbf{V}_n \\ \mathbf{U}_{n+1} &= \bar{\Psi}\mathbf{V}_{n+1} + \bar{\Psi}_o\mathbf{V}_n + \mathbf{J}\mathbf{U}_n \\ \mathbf{M}\mathbf{A}_{n+1} &+ \mathbf{C}\mathbf{V}_{n+1} + \mathbf{K}\mathbf{U}_{n+1} = \mathbf{F}_{n+1} \end{aligned} \tag{14}$$

Like the Newmark-β method, the system of algebraic equations for time stepping numerical integration can be solved by several procedures such as acceleration-form or displacement-form. The algorithm of acceleration-form is summarized as shown below.

i) Calculate $\mathbf{a}_o$ *such that* $\mathbf{m}\mathbf{a}_o + \mathbf{c}\mathbf{v}_o + \mathbf{k}\mathbf{u}_o = \mathbf{f}_o$

Set $\mathbf{A}_o = \{\mathbf{0}^T, \mathbf{0}^T, \cdots, \mathbf{0}^T, \mathbf{a}_o^T\}^T$

$\mathbf{V}_o = \{\mathbf{0}^T, \mathbf{0}^T, \cdots, \mathbf{0}^T, \mathbf{v}_o^T\}^T$

$\mathbf{U}_o = \{\mathbf{0}^T, \mathbf{0}^T, \cdots, \mathbf{0}^T, \mathbf{u}_o^T\}^T$

ii) Calculate $\mathbf{M}^{eff} = \mathbf{M} + \mathbf{C}\bar{\Psi} + \mathbf{K}\bar{\Psi}^2$ *and* $\mathbf{M}^{eff^{-1}}$

iii) Do n=0

Set $\tilde{\mathbf{U}}_{n+1}^{(\mathbf{a})} = \bar{\Psi}\bar{\Psi}_o\mathbf{A}_n + (\bar{\Psi}\mathbf{J} + \bar{\Psi}_o)\mathbf{V}_n + \mathbf{J}\mathbf{U}_n$

$\tilde{\mathbf{V}}_{n+1}^{(\mathbf{a})} = \bar{\Psi}_o\mathbf{A}_n + \mathbf{J}\mathbf{V}_n$

Calculate $\mathbf{R}_{n+1}^{(\mathbf{a})} = \mathbf{F}_{n+1} - \mathbf{C}\tilde{\mathbf{V}}_{n+1}^{(\mathbf{a})} - \mathbf{K}\tilde{\mathbf{U}}_{n+1}^{(\mathbf{a})}$

$\mathbf{A}_{n+1} = \mathbf{M}^{eff^{-1}}\mathbf{R}_{n+1}^{(\mathbf{a})}$

$\mathbf{U}_{n+1} = \tilde{\mathbf{U}}_{n+1}^{(\mathbf{a})} + \bar{\Psi}^2\mathbf{A}_{n+1}$

$\mathbf{V}_{n+1} = \tilde{\mathbf{V}}_{n+1}^{(\mathbf{a})} + \bar{\Psi}\mathbf{A}_{n+1}$

Set $n = n+1$

Continue

Moreover, from the stability analysis of a single degree of freedom system that excludes the damping and the applied loading condition, it is known that the present algorithm is unconditionally stable for all the approximation orders. The numerical test about stability is shown in the next section.

III. Numerical Tests for Accuracy Analysis

1. Period Elongation and Accuracy

The percentage error of period elongation e_{period} can be defined by the difference of the numerial period T_{num} and the exact period T as

$$e_{period} = \frac{T_{num} - T}{T} \times 100 \qquad (15)$$

To obtain the period elongation error of the present method, the spring-mass system is chosen and its free-oscillating response is simulated by each order of approximation for various time steps Δt. In this fundamental system, the period elongation is clearly observed. The equation of motion of the model problem is described by

$$ma + ku = 0 \qquad (16)$$

with the initial conditions $u(0) = u_o$ *and* $v(0) = v_o$

where m and k denotes mass and stiffness, respectively and a, v, and u denote acceleration, velocity, and displacement, respectively. From the predicted results, the numerical period is acquired for each order of approximation. The percentage error of period elongation versus $\Delta t/T$ is shown in Fig.1. From Fig.1, it can be known that the present method of the higher order approximation is much more accurate than the trapezoidal rule(the present 1st order approximation). In Fig.2, the percentage period elongation error versus $\Delta t/T$ is plotted in log-scale to observe the order of accuracy of the present method for each order. The slope of each line in Fig.2 indicates the order of accuracy of the proposed method. The result shows that the present method of α-th order approximation is 2α-order accurate.

2. Numerical Examples

2.1 *Free Oscillating Case*

The time domain response of the free-oscillating system is obtained for each approximation order. The system with initial displacement(m=k=1, $u(0) = 1$ and $v(0) = 0$) is solved in Fig.3 and the time domain response of the system with the initial velocity(m=k=1, $u(0) = 0$ and $v(0) = 1$) is simulated in Fig.4. In the simulations, the time steps $\pi/3$, $2\pi/3$, π, and $4\pi/3$ are used for the 1st, 2nd, 3rd, and 4th order approximations, respectively. In spite of the fact that the larger time steps are chosen for the higher order approximations, the more accurate solutions are obtained in the higher order approximations. In particular, the third and the fourth order approximations show the dramatical improvements in the solution accuracy although the time steps of larger than the half of the period are used. Fig.5 shows that the stable solutions are produced for all the orders of approximation with very large time steps compared to system period.

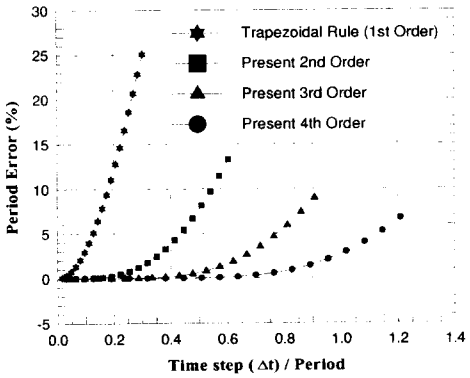

Fig. 1 Percentage period error versus time step for various oders of approximation

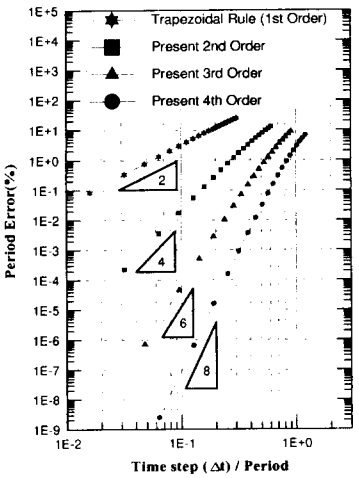

Fig. 2 Log-scale plot of percentage period error versus time step for each order

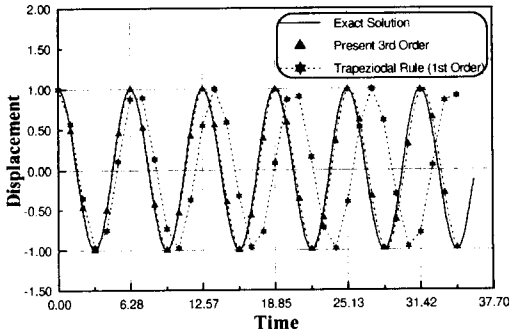

Fig. 3(a) Predicted result of the present method compared to the exact solution for the free-oscillating case using the third order of approximation with zero initial velocity

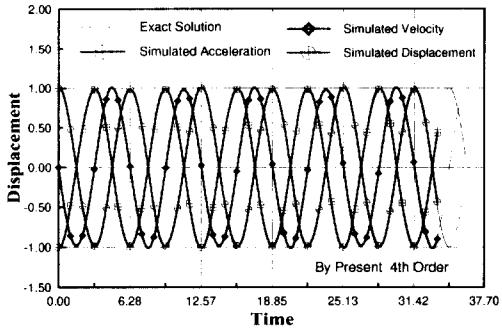

Fig. 3(b) Predicted displacement, velocity, and acceleration by the present method of the fourth order approximation.

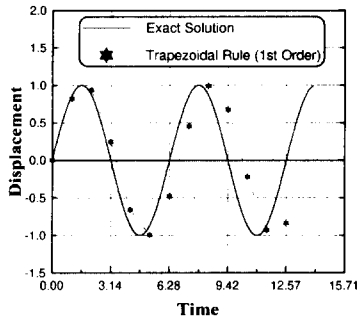

(a) by the first order

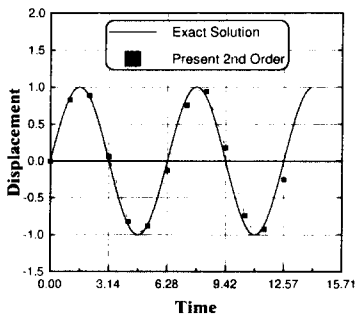

(b) by the second order

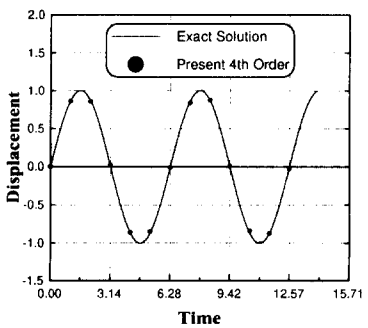

(c) by the fourth order

Fig. 4 Predicted result of the present method using various orders of approximation

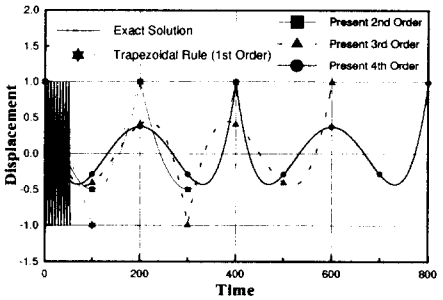

Fig. 5 The simulated solutions with very large time steps compared to the exact period

2.2 *Damped Oscillating Case*

A damped oscillating system is simulated to observe the damping characteristics of the present method. The equation of motion is as follows

$$ma + cv + ku = 0 \qquad (17)$$

with the initial conditions $u(0) = u_o$ *and* $v(0) = v_o$

where c denotes damping coefficients.

The simulations for case $m = k = 1$, $c = 0.2$, $u(0) = 0$ and $v(0) = 1$ are performed by the first and third order approximations. In the numerical calculations, the time steps $\pi/3$ and π are used for the 1st and 3rd order approximations, respectively. The results are shown in Fig.6. Like as the free-oscillating case, the better result is obtained in the higher order approximation. From the example, it can be known that present method predicts the damped motion of the dynamic system very accurately.

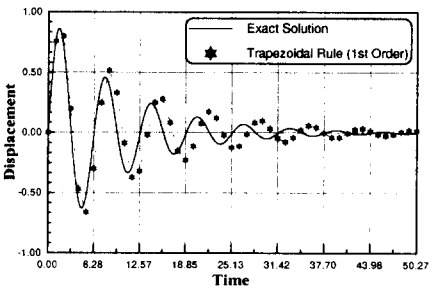

(a) by the first order

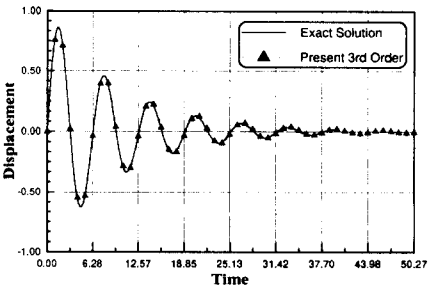

(b) by the third order

Fig. 6 Predicted result for the damped oscillating case using various orders of approximation

2.3 *Forced Vibrating Case*

Forced vibrational motion with no damping is predicted in the third example. The equation of motion assumes the form as follows.

$$ma + ku = f \tag{18}$$

with the initial conditions $u(0) = u_o$ *and* $v(0) = v_o$

The case of $m = k = 1$, $f = -10\sin(0.3t)$, $u(0) = 1$ and $v(0) = 1$ is simulated and the predicted results are compared with the exact solution. The time steps Δt used in the 1st and 4th order approximations are 1 and 4, respectively. Fig.7 shows the simulated results. In the trapezoidal rule (the 1st order approximation), a smaller time step is used than in higher order approximations; nevertheless, the result of trapezoidal rule shows considerable deviation from the exact solution. By comparison it shows the better accuracy of the present method of higher order approximation.

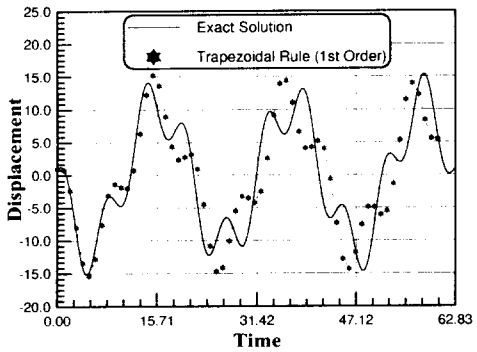

(a) by the first order

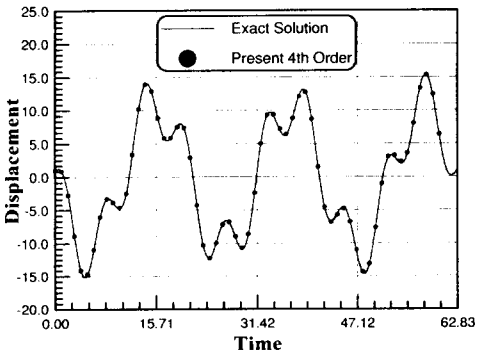

(b) by the fourth order

Fig. 7 Predicted result of the present method compared to the exact solution for the forced vibrating case

2.4 *Vibration of Clamped Euler Beam*

In our final example, the vibrational motion of the clamped Euler beam is analyzed. The governing equation is as follows.

$$\rho A\frac{\partial^2 u}{\partial t^2} + \frac{\partial^2}{\partial x^2}\left(EI\frac{\partial^2 u}{\partial x^2}\right) = f(x,t) \tag{19}$$

with the boundary conditions $u(0,t) = 0$,

$$\left.\frac{\partial u}{\partial x}\right|_{x=0} = 0, \left.EI\frac{\partial^2 u}{\partial x^2}\right|_{x=l} = 0, \left.\frac{\partial}{\partial x}\left(EI\frac{\partial^2 u}{\partial x^2}\right)\right|_{x=l} = 0$$

and the initial conditions $u(x,0) = u_o(x)$ *and* $v(x,0) = v_o(x)$

where ρA, EI, and l are the mass per unit length, the bending stiffness of the beam, and the length of the beam, respectively. The material constants and dimensions of the model used in the simulations are shown below.

Density $\rho = 0.1$ lb / in^3,
Beam cross section area $A = 1$ in^2,
Young's modulus $E = 1\times10^7$ psi,
Moment of inertia $I = 1/12$ in^4,
Length of the beam $l = 20$ in

In the simulations of Fig.8 and Fig.9, 10 conventional 2-node hermite elements of size 2 are used for the space discretization of the beam. With zero initial velocity, the static deflection of the beam due to the tip loading 10 lb is used for the initial displacement. The whole space-time behavior of the beam is shown in Fig.8 which is simulated by the 2nd order approximation with time step $2\pi/1000$ sec.

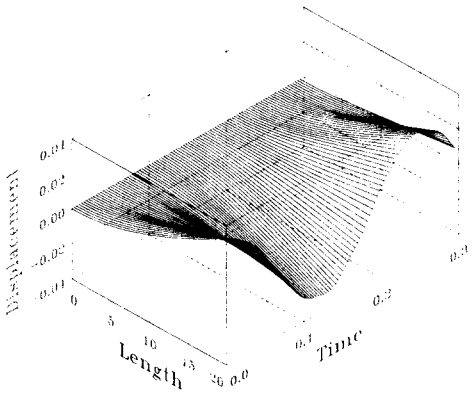

Fig. 8 The whole space-time domain response of Euler beam obtained from the second order of approximation

Fig.9 uses time steps $2\pi/125$ sec, $4\pi/125$ sec, $6\pi/125$ sec, and $8\pi/125$ sec for the time stepping procedures of the 1st, 2nd, 3rd, and 4th order approximations, respectively. The solution for the trapezoidal rule(the present 1st order approximation) with time step $2\pi/12500$ sec is also presented in Fig.9. In

Fig.9, the time dependent responses at the tip of the beam are presented for all the orders of approximation. As previous examples, the accuracy of solution is greatly improved as the approximation order is increased. Finally, the dynamic response due to impulse tip loading $\delta(l,0)$ is simulated with zero initial condition by the third order approximation. In the simulation, the same number of beam elements in Fig.8 is used with several time steps($2\pi/10000$ sec, $2\pi/500$ sec, and $2\pi/50$ sec) . The effect of impulse loading is imposed through the initial velocity since the impulse loading produces an instantaneous change in the velocity. The simulated result of Fig.10 shows that the solutions with large time steps are not deteriorated by higher modes in the stiff systems[12] and stabilized. It is confirmed that the present method conforms well to the stiff systems frequently occurred in structural dynamics.

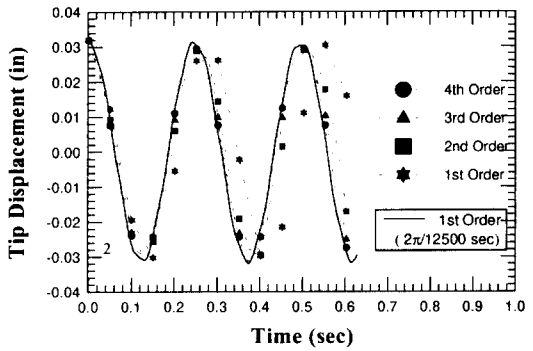

Fig. 9 The tip displacement of Euler beam versus time for each order of approximation with zero initial velocity

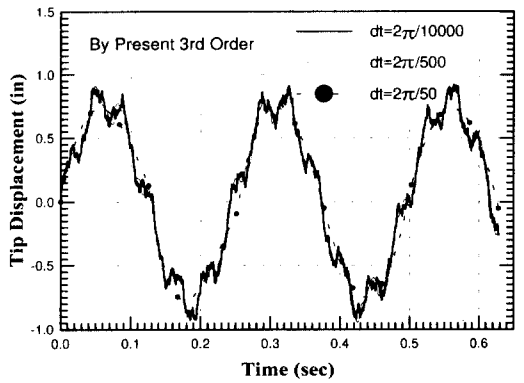

Fig. 10 The tip displacement of Euler beam versus time for various time steps under impulse tip loading condition using the third order approximation

IV. Conclusions

In this work, a new numerical time integration method is developed for the structural dynamics, which is higher order accurate and unconditionally stable. The method is a generalized version of the famous trapezoidal rule. To generalize the concepts of the trapezoidal rule, the projection operator in function space is chosen and averages of higher order acceleration and velocity are obtained. By the procedure, the method uses acceleration and velocity that is averaged in a generalized sense (projection) like the trapezoidal rule. The present method of linear approximation is exactly the same as the trapezoidal rule.

To observe the accuracy of this method, the period elongation error is plotted. The results shows that the present method of α-th order approximation is 2α-order accurate. From the several numerical tests, it can be confirmed that the present method gives unconditionally stable solution, having higher order accuracy and it is justified that the method conforms well to stiff systems frequently occurred in structural dynamics.

References

[1] N. M. Newmark, "A Method of Computation for Structural Dynamics, " *Journal of the Engineering Mechanics Division*, ASCE, Vol. 85, 1959, pp. 67-94.

[2] J. C. Houbolt, "A Recurrence Matrix Solution for the Dynamic Response if Elastic Aircraft, " *Journal of Aeronautical Science*, Vol. 17, 1950, pp. 540-550.

[3] E. L. Wilson, I. Farhoomand, and K. J. Bathe, "Nonlinear Dynamic Analysis of Complex Structures," *International Journal of Earthquake Engineering and Structural Dynamics*, Vol. 1, 1973, pp. 241-252.

[4] H.M. Hilber, T.J.R. Hughes, and R.L.Taylor, "Improved Numerical Dissipation for Time Integration Algorithms in Structural Mechanics, " *International Journal of Earthquake Engineering and Structural Dynamics*, Vol. 5, 1977, pp. 283-292.

[5] K. C. Park, "Evaluating Time Integration Methods for Nonlinear Dynamic Analysis, " pp.35-58 in *Finite Element Analysis of Transient Nonlinear Behavior*, eds. T. Belytschko et al., AMD 14. New York: ASME, 1975.

[6] G. M. Hulbert and T. J. R. Hughes, "Space-Time Finite Element Methods for Second-Order Hyperbolic Equations," *Computer Methods in Applied Mechanics and Engineering*, Vol. 84, 1990, pp. 327-348.

[7] O. C. Zienkiewicz and R. L. Taylor, *The Finite Element Method*, 4th Ed., McGraw-Hill, New York, 1991, Chapter 10.

[8] K. J. Bathe, *Finite Element Procedures*, Prentice-Hall, Englewood Cliffs, NJ, 1996.

[9] G. Dahlquist, "A Special Stability Problem for Linear Multistep Methods, " *BIT*, Vol. 3, 1963, pp.27-43.

[10] J. T. Oden, *Applied Functional Analysis*, Prentice-Hall, Englewood Cliffs, NJ, 1979.

[11] D. G. Luenberger, *Optimization by Vector Space Methods*, John Wiley and Sons, New York, 1969.

[12] G. Strang, *Introduction to Applied Mathematics*, Wellesley-Cambridge Press, Wellesley, MA, 1986.